J. Biomechanics, 1974, Vol. 7, pp. 497–507. Pergamon Press. Printed in Great Britain

A MODEL FOR STUDIES OF MECHANICAL INTERACTIONS BETWEEN THE HUMAN SPINE AND RIB CAGE*†

THOMAS ANDRIACCHI, ALBERT SCHULTZ, TED BELYTSCHKO and JORGE GALANTE‡

Department of Materials Engineering, University of Illinois at Chicago Circle, Chicago, Illinois 60680, U.S.A.

Abstract—A three-dimensional mathematical model useful for studies of the mechanics of the human skeletal thorax is described. To construct this model, rib cage elements are incorporated into a previously reported model of the thoracolumbar spine. The vertebrae and bony portions of the ribs and sternum are idealized as rigid bodies. The behavior of the discs, ligaments and costal cartilages are modelled by deformable elements. Appropriate geometric and stiffness property data are assigned to the elements of the model. In constructing the model, it was found that the mechanical response of the costo–vertebral joint is strongly influenced by articulation geometry. Although rigid bodies were used to model calcified portions of the ribs, the model predicted rib cage deformations in close agreement with those measured experimentally. These studies indicate that the rigid body motion of calcified portions of the rib makes a major contribution to the deformation of the rib cage in response to certain types of loadings. Quantitative results are also reported on the roles the rib cage plays in bending responses of the spine, the lateral stability of the spine, and the production and correction of several scoliotic deformities.

1. INTRODUCTION

An understanding of the mechanics of the human thorax is fundamental to any explanation of its normal or pathological behavior. The skeletal thorax is subjected to muscle forces, the forces of weight bearing and externally applied loads. A detailed study of the mechanisms of force transmission and displacement response is a useful first step to a quantitative explanation of its behavior. For example, consider the mechanisms which contribute to the lateral stability of the spine. Lucas and Bresler (1961) found experimentally that the isolated ligamentous thoracolumbar spine is capable of supporting only a 2 kp compressive load before buckling. *In vivo*, the spinal column is capable of supporting much larger loads. The rib cage contributes to the stability of the *in vivo* spinal column, but to an unknown degree. A more complete understanding of the role the rib cage plays in stabilizing the spinal column would be important. An understanding of the mechanics of the thorax is also important in studies of chronic back injury, crash injury protection and the treatment of scoliosis.

Fletcher (1971) used a simple mathematical model to determine the response of the thorax to air blast loading and Roberts and Chen (1970) have described a three-dimensional finite element model of the skeletal thorax. This paper introduces a three-dimensional multi-component mathematical model which can be used to study thoracic cage forces and displacements. The work is an extension of a series of investigations concerned with the mechanics of the spine. It uses the computational techniques described by Belytschko *et al.* (1973) and considers the addition of rib cage elements to the model of the isolated spine described by Schultz *et al.* (1973).

Section 2 of the paper describes the construction of the model. Section 3 presents the results of several verification studies in which the predicted response of the model was compared with experimentally observed behavior. Section 4 reports findings from several initial investigations conducted using the model.

2. DESCRIPTION OF THE MODEL

General

The model consists of elements which represent the vertebrae of the thoracolumbar spine, the sacrum, rib pairs 1–10, and the sternum. Each of the 17 thoracolumbar vertebrae, the sacrum, the sternum and the calcifed portion of each rib is modelled as a rigid body. These 39 rigid bodies are interconnected by 236 spring-type and 59 beam-type deformable elements which represent the intervertebral discs, joint capsules, costal cartilages and ligaments. The model incorporates

* *Received* 25 *March* 1974.

† This research was supported in part by Public Health Service Grant AM 15575 and Social and Rehabilitation Service Grant 23P 55785.

‡ Department of Orthopaedic Surgery, Rush-Presbyterian–St. Luke's Medical Center, Chicago, Illinois 60612, U.S.A.

many anatomical features, such as the sagittal plane curves of the vertebral column, the complex geometric shape of each vertebra and rib and level to level variations in stiffness of connective tissue.

There are two aspects to the modelling procedure: the computational technique, which involves describing the responses of a general mechanical system by a set of equations, and the description of the physical property data necessary to characterize specific mechanical behavior of the human skeletal thorax.

Computational technique

The computational procedure provides mathematical relationships between the forces and displacements of a mechanical system. The mechanical system consists of a set of rigid bodies in three-dimensional space, which are interconnected by deformable elements. The deformable elements are either spring-type or beam-type elements and can include quasi-linear force–displacement response. The computational technique is capable of treating the geometric non-linearities associated with large displacements and large rotations as well as non-linear material properties.

The solution procedure is numerical, and employs a digital computer, requiring systematic organization of the governing equations in discrete form. The technique is based on the direct stiffness method of structural analysis, and a complete description can be found in Belytschko *et al.* (1973). The three-dimensional motion of the 39 rigid bodies used here to represent the skeletal thorax are described by a coupled system possessing 234 degrees-of-freedom. Solutions of the governing equations sometimes take in excess of 10 min of IBM 370/155 computer time.

Property data: geometry

The shape of the rigid body which represents a vertebra, calcified rib section or sternum is defined by points located relative to a local coordinate system embedded within that body. The local coordinate system moves with its respective body. By defining the location and orientation of each local coordinate system relative to a fixed global system, the location of every point in the model is known.

(a) *Spinal column.* The geometry of the model spine without the rib cage was described in a prior investigation reported by Schultz *et al.* (1973). The geometry of each vertebra was defined in that investigation by 16 points. In the present model it was necessary to place 4 additional points on each thoracic vertebra for the costo–transverse and costo–vertebral articulations.

(b) *Location of costo–transverse and costo–vertebral articulations.* The data reported in Schultz, Benson and Hirsch (1974b) were used to locate the costo–transverse (*CT*) and the superior and inferior costo–vertebral (*CV*) articulations. The diagrams accompanying Table 1 indicate the nature of these data. Table 1 shows the mean values of placement data for

Table 1. Locations on the thoracic vertebrae of points for attachment of costo–vertebral (*CV*) and costo–transverse (*CT*) elements

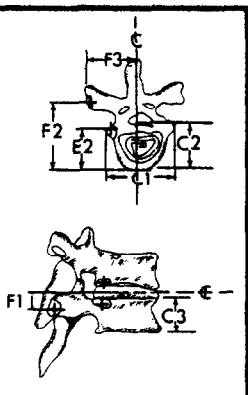

Level	C1*	Inf.+ Trans. Diam.	C2*	Sagittal Diam.+ Sup./Inf.	C3*	Ant.+ Vertical Diam.	E2*	F1*	F2*	F3*
T1		3.16		1.66/1.75		1.62		.030	1.90	4.0
T2	3.03	3.22	2.05	1.79/1.95	1.95	1.77	1.22	.033	3.36	3.81
T3		3.09		2.0/2.18		1.84		.033	3.50	3.0
T4	3.09	3.04	2.47	2.23/2.37	2.07	1.88	1.92	.035	4.70	3.01
T5		3.09		2.42/2.56		1.90		.035	4.73	3.30
T6	3.22	3.20	2.88	2.61/2.73	2.23	1.90	2.45	.035	4.96	3.33
T7		3.34		2.74/2.86		1.89		0.0	4.90	3.30
T8	3.60	3.52	2.98	2.92/3.03	2.45	1.97	2.72	0.0	5.36	3.02
T9		3.74		3.04/3.08		2.06		0.0	5.30	2.80
T10	4.12	4.08	3.22	3.07/3.14	2.55	2.23	3.06	0.0	5.14	2.53

* Mean value of 5 specimen reported in Schultz, Benson and Hirsch (1974b)
\+ Data reported by Lanier (1939) [All data in cm.]

EXPLANATION OF SYMBOLS

C1-Max. lateral diameter
C2-Midline AP diameter
C3-Anterior vertebral body height
E2-Posterior distance from anterior edge of disc to costo-vertebral facet
F2-Posterior distance from anterior edge of disc to costo-transverse facet
F3-Lateral distance from centerline to costo-transverse facet
F1-Superior departure from centerline to costo-transverse facet

Table 2. Locations on the left side of the sternum of seven points of attachment for costal-cartilage (*CC*) elements. Bilateral symmetry assumed for right side

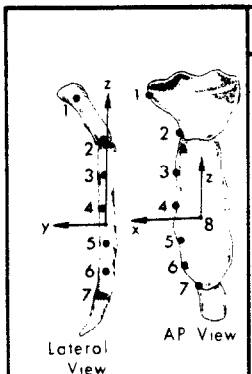

Point No.	Coordinate (cm.) x	y	z
1	- 3.0	6.0	12.0
2	- 2.0	3.7	9.5
3	- 2.1	2.2	5.3
4	- 2.3	0.4	1.3
5	- 2.1	-.3	-.7
6	- 2.0	- 1.0	- 2.5
7	- 1.5	- 1.5	- 4.3
8	0.0	0.0	0.0

5 specimens reported by Schultz, Benson and Hirsch and data concerning vertebral body measurements from the work of Lanier (1939) for comparison. There was good agreement among these data. Lanier's data for the intervening levels was used as a basis for interpolation to provide the remaining *CV* and *CT* location data required to construct the model.

(c) *Sternum geometry*. As with each vertebra, a local coordinate system was placed within the sternum. Since 7 rib pairs usually articulate directly with the sternum, 14 points were located along the lateral borders of the model sternum, 7 on each side, to provide points of attachment for the deformable elements used to represent the costal cartilages. Sternal geometry data were adopted from the measurements reported by Schultz, Benson and Hirsch (1974b) and are shown in Table 2.

(d) *Rib geometry*. The geometry of each rib is characterized by 8 points placed as follows: 2 coincident points lying on the costal tubercle defining the position of the costo-transverse articulation (*CT*) points, a pair of inferior and superior points placed at the rib head at the positions of the costo-vertebral articulation (*CV*) points. 2 points placed along the inferior and superior borders of the rib shaft at the mid-axillary line to provide points of attachment for deformable elements representing the elastic behavior of the soft tissue occupying the intercostal spaces (*IC*) points, and a pair of points at the anterior end of the calcified portion of the rib providing points of attachments for deformable elements representing the costal cartilages.

Rib geometry data were also obtained from measurements reported in Schultz, Benson and Hirsch (1974a). Data describing the rib shaft geometry are reported in Table 3.

(e) *Assembly of rib cage elements*. Once the individual geometry of each of the skeletal components is described, they are assembled in the normal anatomical position. For this purpose, anthropometric data reported by Clauser *et al.* (1969) and Damon *et al.* (1966) were employed to place the sternum and ribs in an anatomical position relative to the vertebral column.

The standing position height of rib 10 (111 cm) was used to place the ribs in the caudo-cranial direction. The substernal height (141 cm) reported by Clauser *et al.* was also used to position the ribs in the global system. Figure 1 shows the resulting normal anatomical position. Triangular flags symbolize spinous processes, rectangular planes indicate mid-pedicle cross-sections and straight lines join left and right side transverse processes.

Property data: material properties

The deformable elements which represent the soft tissues in the model are assumed to exhibit quasi-linear behavior. This provides for differences in behavior in tension and in compression. Deformable element stiffnesses are defined as the ratio of total load to total deformation in the direction of the loading. Two types

Table 3. Rib shaft geometry in a quasi-horizontal plane. Measurements selected from data of Schultz, Benson and Hirsch (1974a) at levels 2, 4, 6, 8 and 10 and interpolated for intervening levels

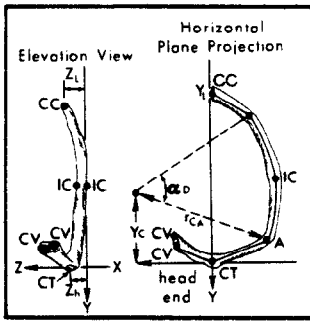

Rib	Y_L cm	Y_A cm	X_C cm	Y_C cm	r_{CA} cm	α_{AD} degrees	Z_H (cm)	Z_L (cm)
1	7.0	-2.5	1.0	- 1.5	11.4	31.0	0.0	0.0
2	1.0	-3.2	5.0	- 1.9	11.0	50.0	0.0	0.0
3	5.4	- 1.2	2.5	- 5.7	9.0	83.0	0.0	0.0
4	6.6	-0.9	2.4	- 5.7	11.0	88.0	0.0	0.0
5	3.3	- .65	6.5	- 8.35	14.5	66.0	0.0	0.0
6	2.4	-2.8	10.5	- 9.8	8.0	57.0	1.05	- 1.0
7	3.2	-2.3	10.6	-10.3	18.0	61.0	.05	- 1.95
8	3.9	- 1.8	0.6	-10.7	18.0	70.0	.05	- 2.9
9	1.4	- 1.3	5.6	- 9.3	13.0	90.0	.1	- 2.5
10	19.8	-0.3	4.9	- 9.1	11.0	105.0	.1	- 2.9

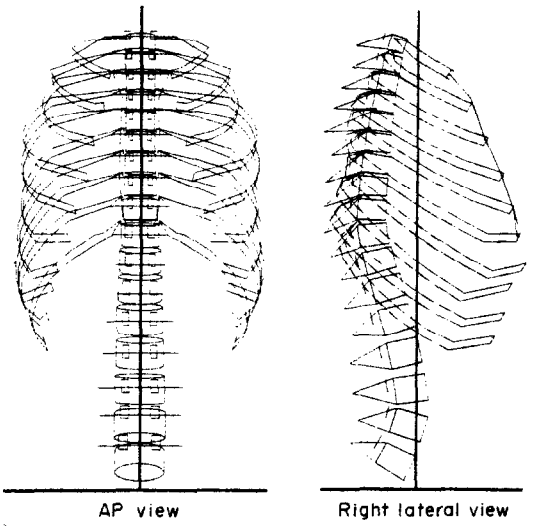

Fig. 1. Computer generated views of lumbar spine and skeletal portions of the thorax in a normal anatomical position.

of deformable elements are used, springs and beams. The beam elements exhibit bending, torsional and shear resistance.

(a) *Spinal column.* Eight spring elements and 1 beam element connect each pair of adjacent vertebrae. The spring elements are: 1 *SP* element between adjacent spinous processes, representing the intra and supraspinous ligaments; 2 *TP* elements between right and left side transverse processes, representing the intertransverse ligaments; 2 *AF* elements joining adjacent articular facets, modelling the kinematic rôle of those joints; 2 *RT* elements representing the ligamenta flava; and 1 *VB* element connecting adjacent vertebral bodies and representing the tension–compression resistance of the disc. The beam element connects adjacent vertebrae and represents the bending, shear and torsional stiffness of the intervertebral disc.

(b) *Costo–vertebral joint.* The behavior of the costo–vertebral joint is modelled so as to represent the kinematic constraints imposed by this joint as well as the resistance to deformation of the connecting ligamentous tissue. As shown in Fig. 2, each of ribs 2–10 is connected by an inferior *CV*, a superior *CV* and a *CT* element. Each *CV* element is a bilinear spring with compressive stiffness ten times as great as its tensile stiffness. The *CT* is a beam element with axial, bending, torsional and shear resistances.

To assign stiffness properties to these elements, the experiments of Schultz, Benson and Hirsch (1974b) were simulated on the computer. A set of trial stiffnesses was assigned to each of the deformable elements of Rib 6, which was isolated from the remainder of the rib cage. Displacements were then computed for five loadings, and the stiffness properties of the elements were successively adjusted until computed displacements satisfactorily agreed with the experimental results of Schultz, Benson and Hirsch as shown in Fig. 2.

This procedure was then repeated at each of the other levels. It was found that the variation between levels in magnitude of the displacements found experi-

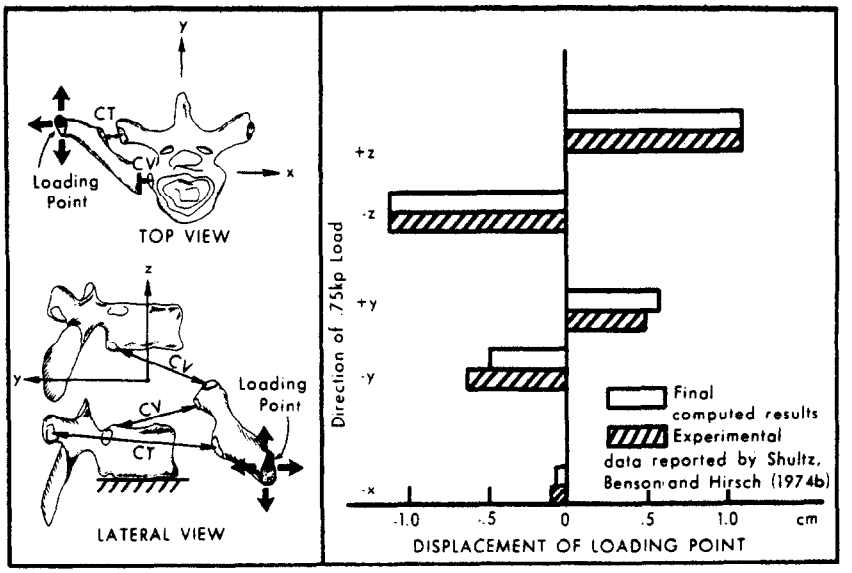

Fig. 2. Illustration of simulation studies for the assignment of stiffness values to the costo–vertebral (*CV*) and costo–transverse (*CT*) elements. Representative results are shown for Rib 6.

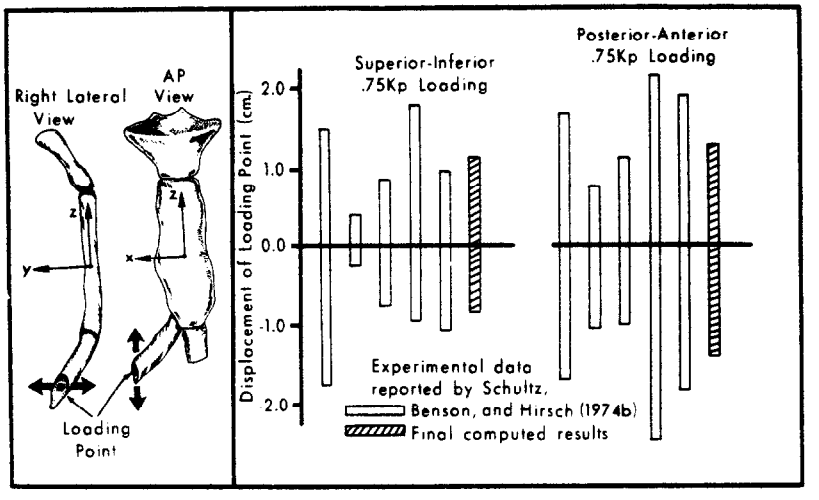

Fig. 3. Illustration of simulation studies for the assignment of stiffness values to costal–cartilage (CC) elements. Representative results are shown for the seventh costal–cartilage.

mentally could be matched solely by differences in articulation geometry. So, the CT and CT stiffness values selected during the Rib 6 tests were used at all levels. This placed the computed displacements at each level well within the range of the experimentally measured values. It appears that rib articulation kinematics are a primary determinant of mechanical behavior.

(c) *Costo–sternal joints, interchondral cartilages, and intercostal elements.* Again, computer simulation of the experiments of Schultz, Benson and Hirsch (1974b) were used to determine the stiffness properties of the deformable elements representing the costal cartilages. A representative set of results are reported in Fig. 3. The elastic behavior of the costal cartilages is represented by a beam-type element (CC) exhibiting axial, bending and torsional stiffness. The CC element connects the calcified portion of the upper seven rib pairs to the sternum. The false ribs are connected to the immediately adjacent ribs by CC elements representing the behavior of the interchondral cartilage. The elastic behavior of the soft tissue occupying the intercostal spaces is represented by a spring-type (IC) element. Representative stiffness values for deformable elements attached to Rib 6 are reported in Table 4.

3. VALIDATION STUDIES

To see if the behavior of the completed model represented the behavior of real rib cages, its response was compared with some available experimental results. Two studies were conducted: the response of the rib cage to lateral loads applied to the lower 5 rib pairs was compared with the results reported by Agostoni *et al.* (1965); and the response of the rib cage to compressive loading on the sternum was compared with experimental results reported by Patrick *et al.* (1966) and Nahum *et al.* (1970). No other data were found that seemed suitable for additional validation studies.

Lateral rib cage loading

Agostoni *et al.* (1965) subjected the relaxed rib cage of live subjects to a lateral squeezing force, and measured the resulting changes in lateral and frontal diameters.

In the simulation procedure the loading was applied along the mid-axillary line, just anterior to the latissimus dorsi muscle and distributed evenly over the lower 5 rib pairs. The sacrum was fixed and T9 constrained from motion in the sagittal plane. Figure 4

Table 4. Stiffness values for deformable elements attached to Rib 6

Element	Axial (kp cm) Tension	Axial (kp cm) Compression	Bending (kp-cm/rad)	Torsional (kp-cm/rad)	Shear (kp/cm)
Inf. CT	5	50	—	—	—
Sup. CT	5	50	—	—	—
CT	5	50	70	100	125
IC	20	20	—	—	—
CC	75	75	25	100	8

shows the experimental and computed changes in lateral diameters at the level of the xiphoid process. which are in good agreement.

The change in lateral diameter computed by the model was due primarily to a rotation of the calcified ribs about an axis in the anteroposterior direction. For example, the lateral diameter at the level of Rib 10 changed by 2·5 cm while the displacement at the rib head was only 0·2 cm.

As shown in Fig. 4 the model underestimated the corresponding changes in frontal diameter due to the lateral squeezing forces. This discrepancy may be partially due to the effects of the intra-thoracic cavity pressure and the thoracic viscera not represented in the model.

Posterior loading of the sternum

To test the response to sagittal plane loading, the experiments reported by Nahum *et al.* and Patrick *et al.* were simulated with the model. With *T*1 and *T*9 fixed in the sagittal plane a compressive load in the anteroposterior direction was applied to the sternum. Anteroposterior displacements were computed for loads up to 12 kp. As can be seen from Fig. 5, the predicted response of the model is in good agreement with experimental results. The following factors contributed to the sternal deflections: deformation of costal cartilage; a 2·5 degree rotation of the rib heads about an axis in the frontal plane at the costo–vertebral articulations; and a 0·1 cm dorsal displacement of the rib head in the sagittal plane.

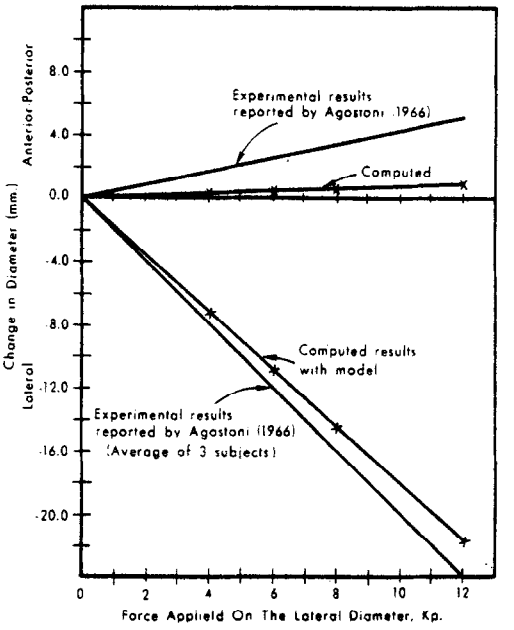

Fig. 4. Model validation study. Computed and experimental changes in lateral and frontal diameters of the rib cage at the level of the xiphoid process in response to a lateral squeezing force applied to lower ribs.

Experimental data concerning the mechanics of the thoracic cage are quite limited. More data are needed in order to fully validate the model. However, based on the results of these two studies, the model appears to be representative. As with any model, it can be only

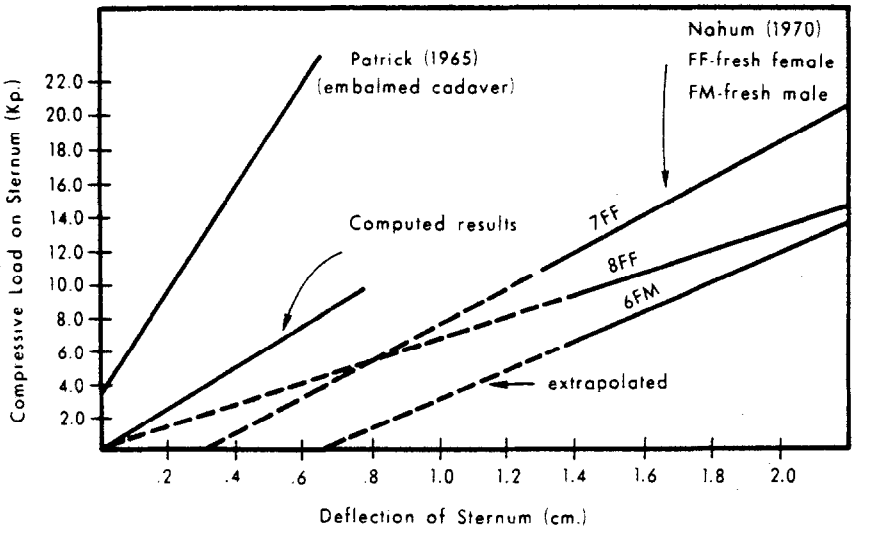

Fig. 5. Model validation study. Computed and experimental deflections of the sternum in response to compressive loading.

Table 5. Stiffening effect of various elements of the rib cage on overall bending stiffness of spinal column. Stiffness determined by dividing applied moment by resulting rotation at T1

Description	Bending stiffness (kp-cm deg) Lateral	Flexion	Extension	Torsion
Isolated spine	0·98	1·69	1·14	1·25
Spine and ribs	1·42	2·14	2·64	1·64
Spine and ribs Intercostals removed	1·31	—	—	
Spine and ribs Sternum removed	0·97	-	-	
Spine and ribs Sternum and intercostals removed	0·97	1·76	1·35	1·28
Spine and ribs Rib 5 resected	1·35	—	—	

partially representative of reality and this limitation should be kept in mind when considering specific applications and results. For example, Lobdell *et al.* (1973) have shown the response to sternal loading of volunteer subjects in a relaxed state differs markedly from their response when the trunk musculature is tensed. The present model does not yet consider muscle forces, and so would not reflect this difference in response. Moreover, although the computational technique allows large displacements and large rotations of the ribs, it would be unrealistic to use this initial model to study situations in which individual ribs experience large loads. At large loads, the calcified portions of individual ribs would deform significantly, and the assumption that the calcified portion of the rib behaves as a rigid body would no longer constitute a valid description of rib behavior.

4. INITIAL STUDIES

Using the model, a series of studies of rib cage mechanics was conducted. The first examined the role of the rib cage in the bending response of the spine. The second investigated the stabilizing effect of the rib cage on the vertebral column, and the third considered the use of the model for study of scoliosis.

Bending response studies

To study the effects of the model rib cage on the bending response of the vertebral column several types of loading were applied to both the isolated spine and the spine with ribs attached. Moments were applied to *T1* to produce lateral bending, flexion, extension and longitudinal twist. The rotational response at each vertebral level was computed. The overall and level by level responses were then compared.

The results reported in Table 5 show the applied moment at *T1* divided by the rotational displacement of *T1* in the direction of that moment, which is indicative of overall stiffness. In each case the rib cage had the effect of increasing this parameter. To illustrate the cage's effect on the bending response of the vertebral column on a level by level basis, the results for the case of lateral bending are shown in Fig. 6. The data were compiled by dividing the relative rotation at each vertebral level by the total applied moment at *T1*. The lateral bending results illustrated in Fig. 6 are representative of the findings for torsion, flexion and extension. The rib cage had the effect of stiffening the motion segments at each level of the thoracic spine.

To isolate the elements of the cage which contributed to these changes in the bending response of the spinal column, systematic changes were made among the elements of the thorax as follows: intercostal elements were removed; intercostals were replaced and the sternum removed; intercostals and sternum were removed; and Rib 5 was resected on both sides.

The response for each of the above situations is compared to the response of the isolated spine and the spine with rib cage intact in Table 5. The removal of the sternum had the greatest effect on the spinal column's bending responses. In removing the sternum the right and left section of the cage were separated anteriorly. An analog can be drawn between the bending behavior of an open thin-walled cylinder and the response of the thorax when the sternum is removed. In both cases the ability to resist bending is markedly increased when the continuity of the cross-section is restored.

To resect Rib 5, the *CT* and *CT* elements were removed on both left and right sides while all *CC* elements were left intact. Table 5 shows the resection of Rib 5 had little effect on the vertebral column's response to lateral bending. This effect has been observed clinically. During corrective surgery for scoliosis it has been found that resecting ribs at one or two levels has little effect on the mobility of the spine.

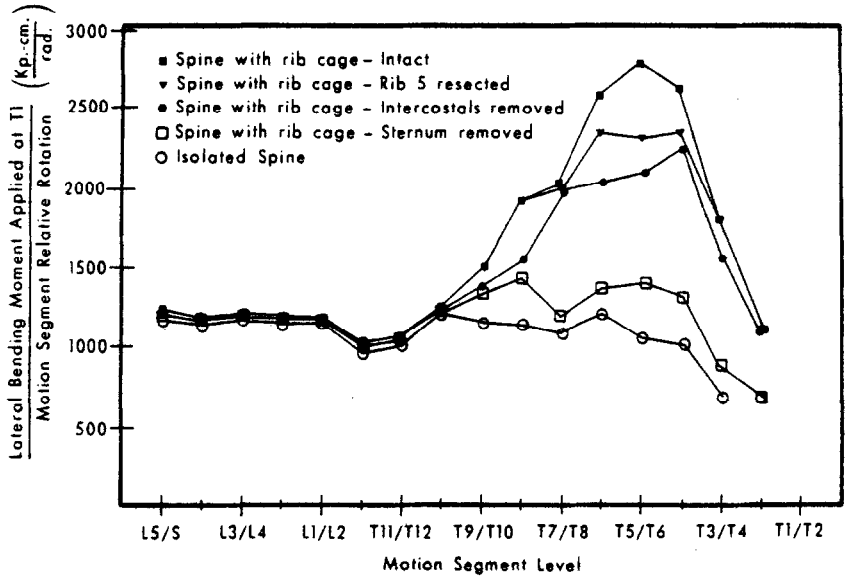

Fig. 6. The contributions of various elements of the thorax to the lateral bending response of each motion segment level.

These studies indicated that:

(1) The rib cage has a significant role in all modes of bending of the thoracic spine;
(2) This role is clearly dependent upon the interaction of the right and left sides of the cage;
(3) The resection of one or two ribs has little effect on the bending response of the overall column.

Stability studies

It has been shown in the experiments of Lucas and Bresler that the isolated spine with *T*1 unconstrained will buckle laterally under a compressive load of less than 2 kp. Belytschko *et al.* (1973) simulated the experiments of Lucas and Bresler in the model of the isolated spine. For each of the constraint conditions on *T*1 the buckling values computed by the model were in good agreement with those found experimentally.

To investigate the role of the rib cage in stabilizing the spinal column the same experiments were simulated in the spine with rib cage attached, and the results are also reported in Table 6. For each of the constraint conditions the rib cage had the effect of increasing the buckling load of the thoraco–lumbar vertebral column by a factor of three to four. So the rib cage stabilizes the spine considerably, but still other factors must be involved in that stabilization. Buckling loads *in vivo* are still well above those found in these model studies. An anteroposterior view of a buckled configuration for one case is shown in Fig. 7.

Studies of scoliosis

Scoliosis is characterized by a lateral deviation of the spine with a characteristic concurrent horizontal plane rotation of the vertebral bodies. This complex

Table 6. Stabilizing effect of rib cage on isolated spine for various constraints

	Lateral buckling loads (kp)					
	*T*1 free		*T*1 fixed in *x-, y- and θ_z-directions		*T*1 fixed in all but z*-directions	
	Exp.†	Computed	Exp.†	Computed	Exp.†	Computed
Isolated spine	2·09	2·1	17·1	21·0	33·4	33·0
Spine and rib cage intact	*NA*	8·0	*NA*	62·0	*NA*	101·0

* x is medial–lateral direction, y is anterior–posterior direction, and z is caudal–cranial direction, and θ_z is rotation in horizontal plane.

† Experimental results reported by Lucas and Bresler (1961).

NA—not available.

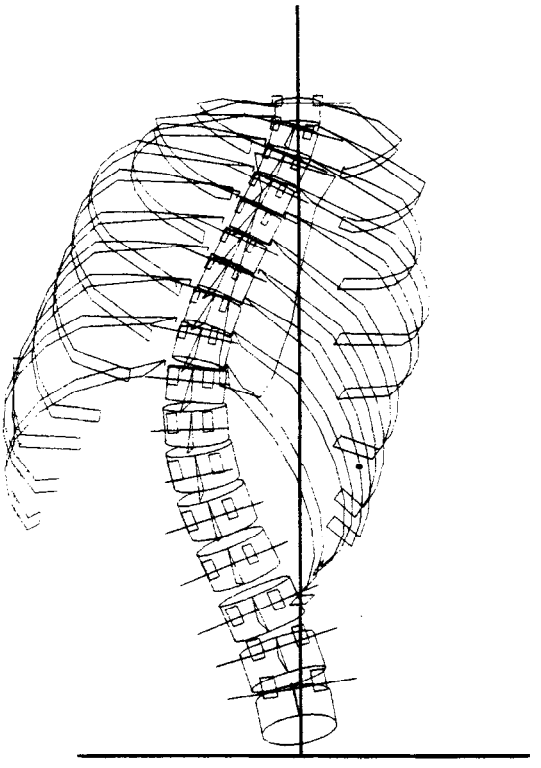

Fig. 7. Computer generated view of a buckled configuration. $T1$ fixed in all but z-directions.

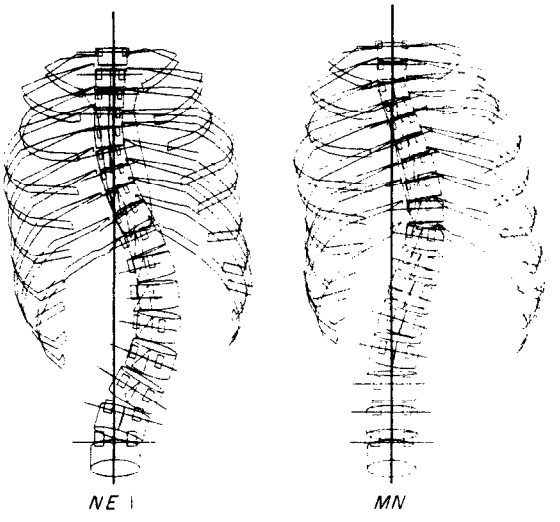

Fig. 8. Computer generated views of $NE1$ and MN model scoliotic configurations.

spinal deformity is usually accompanied by distortion of the rib cage. In some cases, this distortion is of major clinical concern.

To assess the applicability of the present model to the study of scoliosis, several investigations were conducted with the model. The first involved deforming the normal vertebral column with attached rib cage to a configuration representing the deformities found in scoliosis.

The frontal and horizontal plane rotations at each vertebral level were read from radiographs of scoliotic patients. A procedure equivalent to applying a set of moments to each vertebra sufficient to produce these prescribed rotations was carried out and the resulting equilibrium configuration for the spine and ribs was computed. Two scoliotic curves were produced in this manner. The first curve (NE 1) was a 63° right thoracolumbar curve extending from $L4$ to $T5$ and the second (MN) a 40° right thoracic curve from $L1$ to $T4$. In each case $T1$ was constrained not to move laterally or in the sagittal plane. To attain configurations compatible with the radiographs, it was also necessary to constrain Rib 10 on the right and left sides from rotations about axes in the frontal and sagittal planes.

Anteroposterior views of the resulting configurations are shown in Fig. 8. The resulting configurations exhibit qualitatively many of the features found in a scoliotic rib cage. In both the $NE1$ and MN configurations the following characteristics are found: lateral deviation of the vertebral column; frontal and horizontal plane rotations of each vertebra characterizing the deformity; rib cage hump on the convex side of curve; chest wall deformity; and rib drooping, due to imposed constraints on Rib 10.

In the second investigation into the mechanics of a scoliotic rib cage the responses of $NE1$ and MN to lateral bending and to traction were computed. The results were compared to that of a normal rib cage and to the response of the isolated scoliotic spine in the $NE1$ and MN configurations.

For a lateral bending moment applied at $T1$ the response of the scoliotic cage was almost identical to that of the normal rib cage as reported in the section on bending response. The response of the scoliotic cage, normal cage, and isolated scoliotic spines to a tractive

Table 7. A comparison of tractive stiffness of the isolated spine and spine with attached rib cage for normal and scoliotic configurations

Configuration	$\frac{\text{Load at } T1}{\text{Axial displacement}}$ (kp/cm)	
	Isolated spine	Spine and rib cage
Normal	26·6	37·4
$NE1$	13·0	13·8
MN	12·7	15·4

force applied at $T1$ were also computed. Results are reported in Table 7. The rib cage has the effect of stiffening the scoliotic spine in response to tractive force by a factor of about two in comparison to the response of the isolated scoliotic spine. However, the scoliotic spine and rib cage appears only one-third as stiff in response to tractive forces when compared to the normal cage response. Table 7 reports the stiffness in response to a tractive force of 4 kp for each of the normal and scoliotic configurations.

5. DISCUSSION AND SUMMARY

Mathematical modeling employing large high-speed computers has been found to be a useful investigative tool in the study of complex biomechanical systems. This paper has described such a model that can be used to study the mechanics of the skeletal thorax. Through the incorporation of experimental measurements and geometrical data, a representative model has been assembled which accounts for many important mechanical aspects of the skeletal thorax. The model accounts for kinematic and elastic behavior of the joint capsules, cartilages and ligaments. In constructing this model it was found that the kinematic characteristics of the costo–vertebral joint play a major role in determining its mechanical behavior.

The literature was searched for experimental data applicable to validation studies. At present the data available are insufficient to completely validate the model, but they enabled two studies to be conducted which have proven useful. In both validation studies good agreement was found between the model's behavior and experimental data. These experiments examined the various roles of the joints and skeletal elements in the overall response of the rib cage. For example, in the lateral load simulation, the medial–lateral motion of the mid-axillary borders of the rib cage which results from rotation at the costo–vertebral joints was sufficient to predict quite closely the changes in lateral diameter found experimentally. Similarly, the sternal loading experiment validated the costo–vertebral joint and the costal–cartilage properties incorporated into the model.

Since the calcified portion of each rib is assumed to displace as a rigid body, the deformation of the rib cage found experimentally are accounted for solely by the deformation of the costal cartilages and the rigid body motion of the calcified ribs. It should be noted that this description of the rib cage deformation allows relatively large motion of the rib without creating excessively large stresses within the calcified portions. Jordanoglau (1969) concluded that the major contribution to rib cage deformations during tidal breathing is due to a rotation about the neck–head axis. The assumption of rigid motion to represent the major component in the deformations of the calcified rib has proven both useful and reasonable in this model of the skeletal thorax. However, this assumption should not be expected to represent all situations and its applicability must be considered in light of the intended applications of the model.

In exploring the applications of the completed model, a series of preliminary studies has been completed. The results of these studies have led to some useful findings and additional incentives for future investigations. The model indicates that the rib cage plays an important role in the bending response of the vertebral column. For example, in extension, the rib cage increases the bending stiffness of the spine by a factor of two. Similarly, the load bearing capacity of the vertebral column is influenced by the presence of the rib cage. With the addition of the rib cage, the model has shown the isolated spine can support three times as much compressive loading before lateral instability will occur.

The model studies of scoliosis, although preliminary in nature, have also produced some useful findings. The deformities found in the scoliotic rib cage of both $NE1$ and MN, even with calcified portion of the rib assumed rigid, appeared at least qualitatively to possess many of the clinically observed characteristics of a scoliotic cage. This provides a useful starting point for the study of the role of the rib cage in the etiology and correction of this disease. For example, traction applied to the vertebral column is a common correction procedure used in scoliosis. The results in Section 4 show that the rib cage increased the tractive stiffness of the middle thoracic scoliotic spine (MN) by 20 per cent, but the addition of the rib cage had little effect on the tractive stiffness of the lower level scoliotic spine ($NE1$).

As more data become available and through future refinements, the range of the model's applicability will increase. The present model has permitted a first step to be made toward assessing quantitatively the mechanical behavior of the skeletal thorax.

REFERENCES

Agostoni, E., Mognoni, G., Torri, G. and Miserocchi, G. (1966) Forces deforming the rib cage. *Resp. Physiol.* **2**, 105–117.

Belytschko, T., Andriacchi, T., Schultz, A. and Galante, J. (1973) Analog studies of forces in human spine: computational techniques. *J. Biomechanics* **6**, 361–371.

Clauser, C., McConville, J. and Young, J. (1969) Weight volume and center of mass of segments of the human body. AMRL-TR-69-70, Wright–Patterson Air Force Base, Ohio.

Damon, A., Stoudt, H. and McFarland, R. R. (1966) *The Human Body in Equipment Design*. Harvard University Press, Cambridge, Mass.

Fletcher, E. R. (1971) A model to simulate thoracic responses to air blast and impact. Symposium on Biodynamic Models and Their Applications. AMRL-TDR-71-29. Oct. 1970. Paper No. 1.

Jordanoglau, J. (1969) Rib movement in health, kyphoscoliosis, and anleylosing spondylitis. *Thorax* **24**, 407–413.

Lanier, R. (1939) The presacral vertebrae of American White and Negro males. *Am. J. Phys. Anthropol.* **25** (3), 341–420.

Lobdell, T., Kroell, C., Schneider, D., Hering, W. and Nahum, A. (1973) Impact response of the human thorax. In *Human Impact Response* (Edited by King, W. and Mertz, H.), pp. 201–245. Plenum Press, New York.

Lucas, D. and Bresler, B. (1961) Stability of the ligamentous spine. Biomechanics Laboratory Report 40. Univ. of California, San Francisco.

Nahum, A. M., Gadd, C. W., Schneider, D. C. and Kroell, C. K. (1970) Deflections of the human thorax under sternal impact. *International Automobile Safety Conference, Detroit and Brussels*, pp. 797–807.

Patrick, L., Kroell, C. and Mertz, H. (1965) Forces on the human body in simulated crashes. *Proceedings 9th Stapp Car Crash and Field Demonstration Conference*, pp. 237–259.

Roberts, S. and Chen, P. (1970) Elastostatic analysis of the human thoractic skeleton. *J. Biomechanics* **3**, 527–545.

Schultz, A., Belytschko, T., Andriacchi, T. and Galante, J. (1973) Analog studies of forces in human spine: mechanical properties and motion segment behavior. *J. Biomechanics* **6**, 373–383.

Schultz, A., Benson, D. and Hirsch, C. (1974a) Force-deformation properties of human ribs. **7**, 303–309.

Schultz, A., Benson, D. and Hirsch, C. (1974b) Force-deformation properties of human costo-sternal and costo-vertebral articulations. **7**, 311–318.